Vesicle Adsorption and Lipid Bilayer Formation on Glass Studied by Atomic Force Microscopy

Holger Schönherr,*[,†,‡,⊥] Joseph M. Johnson,[†,§] Peter Lenz,[§,#] Curtis W. Frank,[†,‡] and Steven G. Boxer[†,§]

NSF MRSEC Center on Polymer Interfaces and Macromolecular Assemblies (CPIMA), Stanford University, Stanford, California 94305-5025, Department of Chemical Engineering, Stanford University, Stanford, California 94305-5025, and Department of Chemistry, Stanford University, Stanford, California 94305-5080

Received March 17, 2004. In Final Form: September 14, 2004

The adsorption of phosphatidylcholine (PC) vesicles (30, 50, and 100 nm nominal diameters) and of dye-labeled PC vesicles (labeled with 6% Texas Red fluorophore (TR) and encapsulated carboxy fluorescein (CF)) to glass surfaces was studied by contact mode atomic force microscopy in aqueous buffer. These studies were performed in part to unravel details of the previously observed isolated rupture of dye-labeled PC vesicles on glass (Johnson, J. M.; Ha, T.; Chu, S.; Boxer, S. G. *Biophys. J.* **2002**, *83*, 3371−3379), specifically to differentiate partial rupture, that is, pore formation and leakage of entrapped dye, from full rupture to form bilayer disks. In addition, the adhesion potential of PC vesicles on glass was calculated based upon the adhesion-driven flattening of adsorbed vesicles and a newly developed theoretical model. The vesicles were found to flatten considerably upon adsorption to glass (width-to-height ratio of approximately 5), which leads to an estimate for the adhesion potential and for the critical rupture radius of 1.5×10^{-4} J/m^2 and 250 nm, respectively. Independent of vesicle size and loading with dye molecules, the adsorption of intact vesicles was observed at *all* concentrations below a threshold concentration, above which the formation of smooth lipid bilayers occurred. In conjunction with previous work (Johnson, J. M.; Ha, T.; Chu, S.; Boxer, S. G. *Biophys. J.* **2002**, *83*, 3371−3379), these data show that 6% TR 20 mM CF vesicles adsorb to the surface intact but undergo partial rupture in which they exchange content with the external buffer.

Introduction

Supported lipid bilayers are useful as model systems for biological membranes.[2−4] Supported bilayers allow study of membrane constituents in a controlled environment[5−9] and may serve as a platform for biosensors based on naturally existing biomolecules in a milieu that approximates a cell membrane.[10−16]

Vesicle fusion to a substrate is one of the most convenient ways of preparing supported bilayers, as it does not require sophisticated equipment and reliably produces high quality supported bilayers. Following the pioneering work of McConnell and co-workers,[17,18] vesicle fusion has been used to form supported bilayers from various lipids on

* Corresponding author. E-mail: h.schonherr@utwente.nl. Phone: +31-53-489 3170. Fax: +31-53-489 3823.

† NSF MRSEC Center on Polymer Interfaces and Macromolecular Assemblies (CPIMA).

‡ Department of Chemical Engineering.

§ Department of Chemistry.

⊥ Present address: University of Twente, Faculty of Science and Technology and MESA+ Institute for Nanotechnology, Department of Materials Science and Technology of Polymers, P.O. Box 217, 7500 AE Enschede, The Netherlands (h.schonherr@utwente.nl).

Present address: Fachbereich Physik, Philipps-Universität Marburg, 35032 Marburg, Germany (peter.lenz@physik.uni-marburg.de).

(1) Johnson, J. M.; Ha, T.; Chu, S.; Boxer, S. G. Early steps of supported bilayer formation probed by single vesicle fluorescence assays. *Biophys. J.* **2002**, *83*, 3371−3379.

(2) Plant, A. L. Self-Assembled Phospholipid Alkanethiol Biomimetic Bilayers on Gold. *Langmuir* **1993**, *9*, 2764−2767.

(3) Sackmann, E. Supported membranes: Scientific and practical applications. *Science* **1996**, *271*, 43−48.

(4) Groves, J. T.; Boxer, S. G. Micropattern formation in supported lipid membranes. *Acc. Chem. Res.* **2002**, *35*, 149−157.

(5) McConnell, H. M.; Watts, T. H.; Weis, R. M.; Brian, A. A. Supported planar membranes in studies of cell−cell recognition in the immune system. *Biochim. Biophys. Acta* **1986**, *864*, 95−106.

(6) Salafsky, J.; Groves, J. T.; Boxer, S. G. Architecture and function of membrane proteins in planar supported bilayers: A study with photosynthetic reaction centers. *Biochemistry* **1996**, *35*, 14773−14781.

(7) Groves, J. T.; Wulfing, C.; Boxer, S. G. Electrical Manipulation of Glycan-Posphatidyl Inositol-Tethered Proteins in Planar Supported Bilayers. *Biophys. J.* **1996**, *71*, 2716−2723.

(8) Grakoui, A.; Bromley, S. K.; Sumen, C.; Davis, M. M.; Shaw, A. S.; Allen, P. M.; Dustin, M. L. The immunological synapse: A molecular machine controlling T cell activation. *Science* **1999**, *285*, 221−227.

(9) Wagner, M. L.; Tamm, L. K. Reconstituted syntaxin1A/SNAP25 interacts with negatively charged lipids as measured by lateral diffusion in planar supported bilayers. *Biophys. J.* **2001**, *81*, 266−275.

(10) Groves, J. T.; Ulman, N.; Boxer, S. G. Micropatterning of Fluid Lipid Bilayers on Solid Supports. *Science* **1997**, *275*, 651−653.

(11) Jenkins, A. T. A.; Boden, N.; Bushby, R. J.; Evans, S. D.; Knowles, P. F.; Miles, R. E.; Ogier, S. D.; Schönherr, H.; Vancso, G. J. Microcontact printing of lipophilic self-assembled monolayers for the attachment of biomimetic lipid bilayers to surfaces. *J. Am. Chem. Soc.* **1999**, *121*, 5274−5280.

(12) Cremer, P. S.; Yang, T. L. Creating spatially addressed arrays of planar supported fluid phospholipid membranes. *J. Am. Chem. Soc.* **1999**, *121*, 8130−8131.

(13) Groves, J. T.; Mahal, L. K.; Bertozzi, C. R. Control of cell adhesion and growth with micropatterned supported lipid membranes. *Langmuir* **2001**, *17*, 5129−5133.

(14) Fang, Y.; Frutos, A. G.; Lahiri, J. Membrane protein microarrays. *J. Am. Chem. Soc.* **2002**, *124*, 2394−2395.

(15) (a) Morigaki, K.; Baumgart, T.; Offenhausser, A.; Knoll, W. Patterning solid-supported lipid bilayer membranes by lithographic polymerization of a diacetylene lipid. *Angew. Chem., Int. Ed.* **2001**, *40*, 172−174. (b) Morigaki, K.; Schönherr, H.; Frank, C. W.; Knoll, W., Photolithographic Polymerization of Diacetylene-Containing Phospholipid Bilayers Studied by Multimode Atomic Force Microscopy. *Langmuir* **2003**, *19*, 6994−7002.

(16) Cheng, Y. L.; Bushby, R. J.; Evans, S. D.; Knowles, P. F.; Miles, R. E.; Ogier, S. D. Single ion channel sensitivity in suspended bilayers on micromachined supports. *Langmuir* **2001**, *17*, 1240−1242.

(17) Watts, T. H.; Brian, A. A.; Kappler, J. W.; Marrack, P.; McConnell, H. M. Antigen Presentation by Supported Planar Membranes Containing Affinity-Purified I-Ad. *Proc. Natl. Acad. Sci. U.S.A. Biol. Sci.* **1984**, *81*, 7564−7568.

10.1021/la049302v CCC: $27.50
Published on Web 11/17/2004

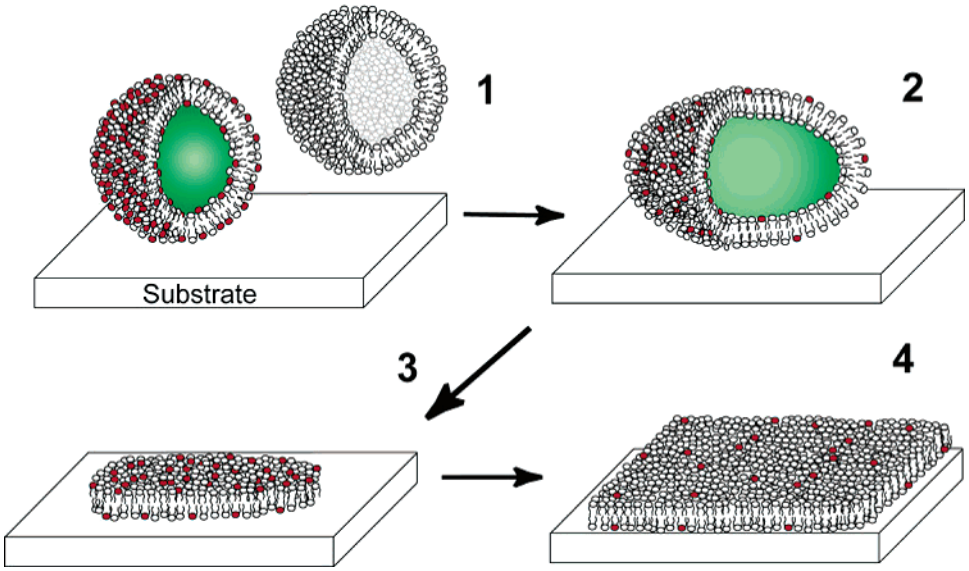

Figure 1. Four step scenario of supported bilayer formation via vesicle fusion comprising (1) vesicle adsorption, (2) fusion of vesicles at the surface to form larger vesicles, (3) rupture of the fused vesicles resulting in bilayer disks, and finally (4) merging of the disks. Here red lipids represent a leaflet fluorophore and green represents an entrapped aqueous dye (ref 1).

substrates, such as glass,[19] mica,[20] self-assembled monolayers,[21] polymers,[22] and quartz.[23]

Much effort has been invested to elucidate the underlying mechanisms of bilayer formation.[1,24−27] A theoretical model has been developed by Seifert and Lipowsky that predicts the dependence of bilayer formation on properties of the vesicles, such as the bending modulus and curvature, along with the adhesive interaction of the vesicles with the solid substrate.[28,29] One central result of this theory is the prediction that only vesicles above a critical size adsorbed on the surface will rupture. The existence of a critical vesicle size of 75 nm has been observed for phosphatidylcholine (PC) vesicles adsorbed to mica by atomic force microscopy (AFM) measurements.[24] Adsorption of intact PC vesicles to glass has been observed by several groups.[1,26,27]

In previous work, the steps of bilayer formation depicted in Figure 1 were investigated using a single vesicle assay based on two color fluorescence microscopy.[1] Fusion was observed by including a self-quenching concentration of Texas Red labeled lipids (TR), and rupture was observed by entrapping soluble carboxy fluorescein dyes (CF) within the vesicles. Four distinct pathways of bilayer formation were observed: (1) primary fusion, as depicted in Figure 1; (2) simultaneous fusion and rupture, in which a labeled vesicle on the surface ruptures simultaneously upon fusion with an unlabeled vesicle; (3) no dequenching, in which loss of fluorescence signal from both dyes occur simultaneously; and (4) isolated rupture (preruptured vesicles), in which a labeled vesicle on the surface spontaneously undergoes content loss, a process that depends on the presence of TR-labeled lipids. The fluorescence signatures alone did not allow differentiation between partial rupture (i.e., pore formation and leakage of entrapped dye) versus full rupture to form a bilayer disk.

Figure 1 depicts a model for the steps of bilayer formation which has emerged from this collective body of theoretical and experimental work: (1) isolated vesicle adsorption to the support surface; (2) fusion of vesicles at the surface to form larger vesicles; (3) rupture of the fused vesicles resulting in bilayer disks; and (4) merging of the disks to form a continuous bilayer.

Isolated rupture events, which may be due to partial rupture or full rupture as discussed above, occurred for approximately 50% of vesicles containing 6 mol % TR. Previously, isolated rupture to form bilayer disks has been reported for vesicles of the same size under similar conditions on mica.[24] To unequivocally differentiate between partial and full rupture for the adsorption of PC vesicles and dye-loaded PC vesicles on *glass* surfaces, we have studied the adsorption behavior of PC vesicles to a glass surface directly by in situ AFM under the same conditions that were used in the single vesicle fluorescence assay. In addition, a new theoretical model was developed, which allowed us to calculate the adhesion potential and the critical rupture radius of the vesicles on the basis of the vesicle dimensions as determined by AFM.

(18) Watts, T. H.; Gaub, H. E.; McConnell, H. M. T-Cell-Mediated Association of Peptide Antigen and Major Histocompatibility Complex Protein Detected by Energy-Transfer in an Evanescent Wave-Field. *Nature* **1986**, *320*, 179−181.
(19) Groves, J. T.; Boxer, S. G. Electric-Field-Induced Concentration Gradients in Planar Supported Bilayers. *Biophys. J.* **1995**, *69*, 1972−1975.
(20) Mou, J. X.; Yang, J.; Shao, Z. F. Atomic-Force Microscopy of Cholera-Toxin B-Oligomers Bound to Bilayers of Biologically Relevant Lipids. *J. Mol. Biol.* **1995**, *5*, 507−512.
(21) Williams, L. M.; Evans, S. D.; Flynn, T. M.; Marsh, A.; Knowles, P. F.; Bushby, R. J.; Boden, N. Kinetics of the unrolling of small unilamellar phospholipid vesicles onto self-assembled monolayers. *Langmuir* **1997**, *13*, 751−757.
(22) Jenkins, A. T. A.; Hu, J.; Wang, Y. Z.; Schiller, S.; Förch, R.; Knoll, W. Pulsed plasma deposited maleic anhydride thin films as supports for lipid bilayers. *Langmuir* **2000**, *16*, 6381−6384.
(23) Kalb, E.; Frey, S.; Tamm, L. K. Formation of Supported Planar Bilayers by Fusion of Vesicles to Supported Phospholipid Monolayers. *Biochim. Biophys. Acta* **1992**, *31*, 307−316.
(24) Reviakine, I.; Brisson, A. Formation of supported phospholipid bilayers from unilamellar vesicles investigated by atomic force microscopy. *Langmuir* **2000**, *16*, 1806−1815.
(25) Keller, C. A.; Glasmastar, K.; Zhdanov, V. P.; Kasemo, B. Formation of supported membranes from vesicles. *Phys. Rev. Lett.* **2000**, *84*, 5443−5446.
(26) Keller, C. A.; Kasemo, B. Surface specific kinetics of lipid vesicle adsorption measured with a quartz crystal microbalance. *Biophys. J.* **1998**, *75*, 1397−1402.
(27) Reimhult, E.; Hook, F.; Kasemo, B. Vesicle adsorption on SiO_2 and TiO_2: Dependence on vesicle size. *J. Chem. Phys.* **2002**, *117*, 7401−7404.
(28) Lipowsky, R.; Seifert, U. Adhesion of Vesicles and Membranes. *Mol. Cryst. Liq. Cryst.* **1991**, *202*, 17−25.
(29) Seifert, U. Configurations of fluid membranes and vesicles. *Adv. Phys.* **1997**, *46*, 13−137.

Experimental Section

Materials. Egg phosphatidylcholine (egg PC) was purchased from Avanti Polar Lipids (Alabaster, AL). Texas Red 1,2-dihexadecanoyl-*sn*-glycero-3-phosphoethanolamine, triethylammonium salt (TR) and 5-(and-6)-carboxyfluorescein mixed isomers (CF) were purchased from Molecular Probes (Eugene, OR). Glass coverslips (no. 1.5) were purchased from VWR (Westchester, PA).

Vesicle Preparation. Extruded unilamellar vesicles (referred to simply as vesicles) were prepared according to the protocol described in Johnson et al.[1] Briefly, chloroform was evaporated from the egg PC under a vacuum, and the lipids were then allowed to hydrate in standard buffer (10 mM Tris [pH 8], 100 mM NaCl). The resulting multilamellar vesicles were subjected to 5 freeze/thaw cycles and then extruded through polycarbonate membranes of 30, 50, or 100 nm pore diameter (Avanti Mini-Extruder). The vesicle sizes quoted in this paper refer to the pore size used for extrusion. The vesicle size distribution was not independently measured; however, the conclusions drawn do not depend on knowing vesicle sizes in solution. For labeled vesicles, TR was mixed with egg PC in chloroform; the mixture was dried and resuspended in a solution of 20 mM CF dissolved in 10 mM Tris [pH 8] buffer with the appropriate amount of NaCl to make the solution iso-osmolar (intravesicular solution: 20 mM CF, 10 mM Tris [pH 8] equilibrated with 50 mM NaOH, 65 mM NaCl) with the standard buffer. Vesicles were generally prepared at a nominal lipid concentration of ~5 mg/mL and subsequently diluted before experiments. TR-labeled vesicles with encapsulated dyes were separated from external dyes by eluting through a Sepharose CL-4B column equilibrated with standard buffer (extravesicular solution: 10 mM Tris [pH 8], 100 mM NaCl). Vesicles were generally used within 1 day of preparation, and external dyes were removed on the day of the experiment.

Substrate Preparation. Glass coverslips were prepared by soaking the substrates in heated detergent solution (Linbro 7X Lab Glass Cleaner, ICN Pharmaceuticals) for at least 20 min, followed by exhaustive rinsing. The coverslips were then baked at 400 °C for 4 h. The root-mean-square (rms) roughness of the substrates prepared following this procedure was 0.3 ± 0.1 nm as determined by contact mode AFM in water ($(5\ \mu m)^2$ scan size).

Atomic Force Microscopy. The AFM experiments were carried out on a NanoScope III (Veeco/Digital Instruments (DI), Santa Barbara, CA) in contact mode (CM). V-Shaped Si_3N_4 cantilevers were used (Nanoprobes (DI)). The cantilevers had a force constant of $k_c = 0.056$ N/m as calibrated by the reference lever method[30] and tip radii of 20−40 nm estimated from images of a calibration standard (Silicon-MDT, Moscow, Russia). Measurements were performed on baked glass coverslips in buffer (10 mM Tris [pH 8], 100 mM NaCl) or Milli-Q water using a DI liquid cell. The temperature inside the cell was 31−32 °C. The measurement procedure described in ref 15b was followed, with minimized forces (imaging force < 60 pN). After liquid exchange, data were acquired after the photodiode signal showed a constant reading. If necessary the forces were adjusted during each scan by manually minimizing the set point. Typical scan rates of 3−5 Hz at a resolution of 256−512 pixels/line were used. All images shown were subjected to a first order plane-fitting procedure to compensate for sample tilt and, if necessary, to a zeroth order flattening. The cross-sectional analysis was carried out on images subjected only to a first order plane-fitting procedure. Vesicles with a streaked appearance (see below) were not included in the quantitative analysis. The widths were estimated as mean value of the widths obtained from cross-sectional plots through the vesicles for different relative orientations (see Supporting Information, Figure S1).

Results

Vesicles were adsorbed to glass at low surface coverage to allow imaging of individual vesicles by contact mode AFM (Figure 2). Elevated features were observed with sizes that correlated with the nominal diameter of the vesicles in solution. Due to the upper limit of noninvasive

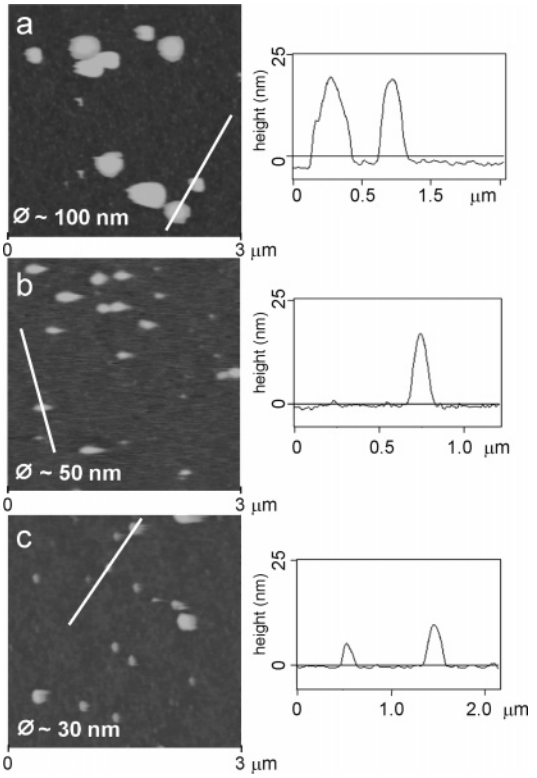

Figure 2. Contact mode AFM height images of vesicles adsorbed on glass and corresponding section analyses (mean vesicle diameters Ø: (a) 100 nm; (b) 50 nm; (c) 30 nm) (vesicle concentration: (a) 5×10^{-4} mg/mL, (b) 5×10^{-4} mg/mL; (c) 5×10^{-3} mg/mL). The gray scale in the images covers a range of 50 nm from dark to bright. Images were obtained in buffer at minimized forces. The section analyses show the profiles along the corresponding lines indicated in the AFM images.

(destructive) imaging forces (<60 pN), tip lift-off frequently made vesicles appear to be streaked in the scanning direction, as opposed to circular. The streaking was observed predominantly for larger vesicles but could be avoided in most cases by choosing appropriate imaging forces and scan rates. For the purpose of investigating the nature of the previously observed partial vesicle rupture upon adsorption to glass, we utilized the lowest possible forces to avoid AFM tip-induced rupture, while for the quantitative determination of the heights and widths of the adsorbed vesicles slightly higher forces and in particular lower scan rates were used to avoid the streaking.

The appearance of the features observed in Figure 2 changed rapidly if imaged under invasive (destructive) imaging conditions. For imaging forces exceeding ~60 pN, insufficient gain, or too rapid scanning, the elevated features changed appearance from one scan line to the subsequent scan line as illustrated in Figure 3. The resulting feature (in the slow scanning direction) was a much flatter elevated patch, with a typical height of 5.0 nm. This height agrees well with the thickness of a complete bilayer, as previously measured by AFM.[31,32] The observed features in Figures 2 and 3 are therefore attributed to adsorbed vesicles, which undergo rupture to form bilayer disks under invasive imaging conditions. By using carefully adjusted set points, the tip-induced rupture

(30) Tortonese, M.; Kirk, M. Characterization of application specific probes for SPMs. *Proc. SPIE* **1997**, *3009*, 53−60.

(31) Egawa, H.; Furusawa, K. Liposome adhesion on mica surface studied by atomic force microscopy. *Langmuir* **1999**, *15*, 1660−1666.

(32) Grandbois, M.; ClausenSchaumann, H.; Gaub, H. Atomic force microscope imaging of phospholipid bilayer degradation by phospholipase A(2). *Biophys. J.* **1998**, *74*, 2398−2404.

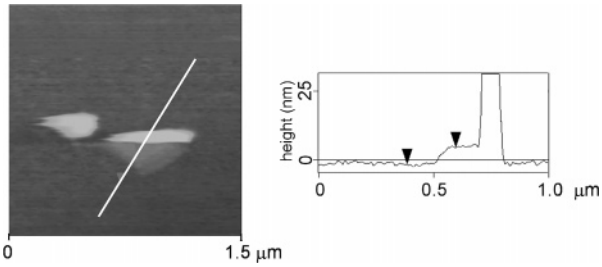

Figure 3. AFM height image (left) and corresponding cross-section analysis (right) of the tip-induced rupture process (scan direction downward). The height difference between bilayer patch and substrate following tip-induced vesicle rupture, as indicated by the markers, is 5.0 nm.

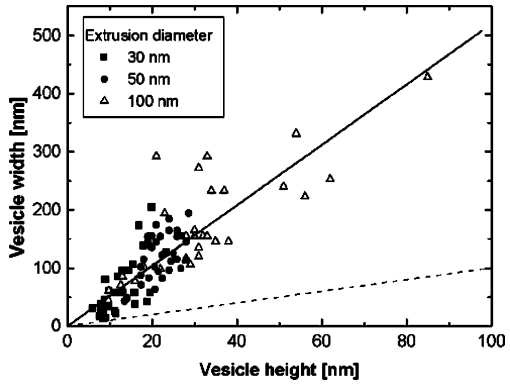

Figure 4. Plot of corrected width vs height of different vesicles adsorbed on glass. The solid line is a linear least-squares fit to the data, giving a slope of 5.2. The dashed line is for comparison; it has a slope of unity as would be expected for the width vs height of vesicles in solution.

could be reliably avoided. AFM tip-induced rupture of adsorbed vesicles has been previously reported.[33]

From these observations,[34] we can infer that vesicles with mean diameters between 30 and 100 nm adsorb *intact* on glass at low vesicle concentrations. We have not observed the adsorption of vesicles from solution or desorption of intact vesicles in real time. Similar observations were also made in the case of 50 nm diameter vesicles with 6% TR and entrapped CF (Supporting Information, Figure S2), which previously showed isolated rupture events for approximately 50% of vesicles.[1] At higher solution concentrations, the surface coverage increases, until at some critical solution concentration ($>6 \times 10^{-3}$ mg/mL) a bilayer is formed.

The lipid bilayer has an almost featureless appearance with an rms roughness of <0.3 nm (glass, <0.4 nm) measured on 1 μm^2. If scratched with the AFM tip, the height of the bilayer is measured to be 4.7 nm. This also allows an estimation of the maximum size of any defects present in the bilayer (see Supporting Information, Figure S3).

A more quantitative analysis of the vesicles shows a linear correlation between measured diameter and height with a nonunit slope (Figure 4). The widths and heights were determined from sectional plots as described in the Experimental Section (see also Supporting Information, Figure S1). For this analysis, we have corrected the measured width by subtraction of the measured tip diameter.[35] We minimize possible flattening of the vesicles

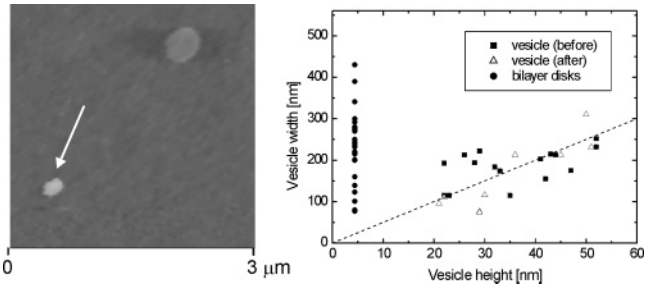

Figure 5. Left: Labeled 50 nm vesicles after osmotic rupturing induced by exchanging buffer with Milli-Q water. In the AFM height image, a bilayer disk can be recognized, as well as an intact vesicle, which is marked by an arrow. The image was acquired in buffer to avoid the effect of double layer repulsion (ref 38). Right: comparison of width vs height for vesicles prior to and after osmotic rupturing, as well as bilayer disks formed as a result of the osmotic shock (the slope of the dashed line is 5.2). All data were obtained under identical imaging conditions in buffer.

as a result of normal forces induced by the AFM tip[36] by using the lowest possible imaging forces (~30 to ~50 pN). An estimate of the indentation length indicates that the flattening can be neglected for the conditions used in our experiments.[37]

The solid line in Figure 4 is a linear least-squares fit of width versus height with a slope of 5.2. The dashed line shows a slope of unity for comparison, which would be the correlation of width versus height for vesicles that adsorbed without flattening. This result is consistent with the view that vesicles adsorb to glass surfaces in a flattened configuration.[28,29]

Labeled vesicles were also observed to rupture in response to osmotic stress. When the buffer solution was replaced with Milli-Q water, many vesicles were found to be ruptured, resulting in isolated bilayer disks. However, we also observed a significant number of vesicles which were stable for hours in salt-free water and did not rupture under these conditions. Intact vesicles were imaged in Milli-Q water, as well as in buffer after exchanging the imaging liquid. The data shown in Figure 5 were acquired in buffer to avoid the effect of double layer repulsion, which may result in height artifacts.[38] The right panel of Figure 5 is a plot of width versus height for adsorbed vesicles and bilayer disks determined in buffer. The bilayer disks show widths from 75 to 425 nm and a height of 4 nm (circles). Adsorbed vesicles before osmotic rupturing (squares) show the same width versus height distribution as adsorbed vesicles that remained intact after osmotic rupturing and exchange of the imaging liquid (triangles).

From the area of each observed bilayer disk following osmotic rupturing, the size of the corresponding original vesicle can be estimated.[39] To within the experimental error, we observe a reasonable correspondence of the mean vesicle diameter estimated from the (deconvoluted) size

(33) Richter, R.; Mukhopadhyay, A.; Brisson, A. Pathways of Lipid Vesicle Deposition on Solid Surfaces: A Combined QCM-D and AFM Study. *Biophys. J.* **2003**, *85*, 3035−3047.

(34) After thermal equilibration, the data for a given set of conditions were acquired within <2 h.

(35) Markiewicz, P.; Goh, M. C. Atomic-Force Microscopy Probe Tip Visualization and Improvement of Images Using a Simple Deconvolution Procedure. *Langmuir* **1994**, *10*, 5−7.

(36) Kumar, S.; Hoh, J. H. Direct visualization of vesicle−bilayer complexes by atomic force microscopy. *Langmuir* **2000**, *16*, 9936−9940.

(37) The indentation length L of a vesicle (with radius $R = 100$ nm) probed by an AFM tip (radius $r = 30$ nm) using a force (F) of 30 pN can be calculated as 1 nm using $L = (R^2F)/(\pi kr^2)$, where k denotes the stretching modulus of the vesicle.

(38) Dufrêne, Y. F.; Barger, W. R.; Green, J. B. D.; Lee, G. U. Nanometer-scale surface properties of mixed phospholipid monolayers and bilayers. *Langmuir* **1997**, *13*, 4779−4784.

(39) Pignataro, B.; Steinem, C.; Galla, H. J.; Fuchs, H.; Janshoff, A. Specific adhesion of vesicles monitored by scanning force microscopy and quartz crystal microbalance. *Biophys. J.* **2000**, *78*, 487−498.

of the observed bilayer patches (estimated diameter = 70 ± 36 nm) and the nominal vesicle size (nominal diameter = 50 nm).

Discussion

In previous work,[1] isolated rupture events were observed for 6% TR vesicles. These events resulted in loss of internal dye signal (CF) from approximately 50% of vesicles adsorbed to glass. These isolated rupture events were not observed for vesicles labeled with 0.5% TR and entrapped CF. In this current work, we have observed that vesicles labeled with 6% TR and containing CF adsorbed intact to glass surfaces, and no isolated bilayer disks resulting from individual vesicles were observed. Thus, the rupture events may be interpreted as exchange of the internal content of vesicles due to an instability, such as pore formation. Transient pore formation has been previously observed in giant vesicles under tension or in contact with black lipid membranes.[40,41] We believe that high TR content and adsorption of the vesicle to the surface destabilize the membrane enough to allow rupture pores to form, but not enough to induce complete rupture of adsorbed vesicles to form bilayer disks.[42]

The measured ratio of width to height shown in Figures 4 and 5 can be used to calculate the strength of the adhesion potential of the glass surface. The experimental values of the width-to-height ratio are compared with those predicted by shape dependent energy functionals as introduced by Lipowsky and Seifert.[28] Generally, the shape of an adhering vesicle is determined by the competition between the free energy cost associated with the curvature elasticity of the membrane and the gain in adhesion energy. The equilibrium shape of adhering vesicles corresponds to the minimum of the free energy functional

$$F = \frac{1}{2}\kappa \int \mathrm{d}A(2H)^2 - WA_{\mathrm{adh}} \qquad (1)$$

where W is the adhesion potential (with units of energy per area), κ the bending rigidity (with units of energy), H the mean curvature (with units of inverse length), and A_{adh} the contact area of the vesicle.[28,29] In determining the minima of eq 1, the volume and area of the vesicle have to be kept fixed.

General solutions of eq 1 are not known. However, in the limit of infinitely strong adhesion $W \rightarrow \infty$ (where curvature energy can be neglected with respect to the adhesion energy) the vesicle shapes can be calculated analytically. In these limits, adhesion of vesicles becomes equivalent to adhesion of conventional liquids on substrates and correspondingly the shape of the vesicles is given by spherical caps, as illustrated in Figure 6.

In this case, the free energy can be written as

$$F_0 = -WA^0_{\mathrm{adh}} + \sigma_0 A + p_0 V \qquad (2)$$

where the area and volume constraint have been explicitly taken into account. Here, σ_0 is the membrane surface tension and p_0 the pressure difference between outside and inside of the vesicle, which act as Lagrange multipliers for the area and volume constraints, respectively. The analogy to conventional wetting can be made more explicit by writing eq 2 as[43]

$$F_0 = (\sigma_0 - W)A^0_{\mathrm{adh}} + \sigma_0(A - A^0_{\mathrm{adh}}) + p_0 V \qquad (3)$$

which is the free energy of a liquid droplet of phase β wetting a flat substrate (γ) in the presence of a vapor phase (α). In this analogy, $\sigma_0 - W$ corresponds to $\Sigma_{\beta\gamma} - \Sigma_{\alpha\gamma}$, σ_0 corresponds to $\Sigma_{\alpha\beta}$, where Σ_{ij} is the interfacial tension between phases i and j, and $p_0 = P_\alpha - P_\beta$ is the pressure difference between outside and inside of the droplet. Thus, the shapes of infinitely strongly adhering vesicles are given by spherical caps with contact angle θ_0 and radius R_0. In eq 1, the curvature contribution is scale invariant whereas the adhesion energy depends on the size of the vesicles. Therefore, the description of vesicles as spherical caps becomes more appropriate for larger vesicles, as the adhesion energy becomes large compared with curvature cost.

It has been shown by Tordeux et al.[43] that the corrections to the limit of infinitely strong adhesion can be calculated analytically for axisymmetric shapes (shapes that are symmetric under rotation around an axis). By introducing the expansion coefficient

$$\epsilon = \frac{1}{L}\sqrt{\frac{\kappa}{W}} \ll 1 \qquad (4)$$

(where L is the radius of the adhesion area of the vesicle), the vesicle shape, its surface area and volume can be calculated in a systematic expansion in ϵ. We expect $\epsilon \approx 0.1$ for vesicles with $\kappa \approx 10kT$ [29] and radius 50 nm adhering to a substrate with $W \approx 10^{-3}$ J/m^2.[24] Thus, higher-order corrections in ϵ should be small, and we can restrict the analysis to first order in ϵ.

Volume V, surface area A, and width ($2L$) to height (h) ratio of the adhering vesicles are then in first order of ϵ given by

$$V = \frac{1}{3}\pi {R_0}^3 \tilde{V}(\theta_0) + O(\epsilon^2) \qquad (5)$$

$$A = \pi {R_0}^2 \tilde{A}(\theta_0) + 2\pi R_0(\delta\tilde{R}(\theta_0)\tilde{A}(\theta_0) + \delta\tilde{\theta}(\theta_0)\sin\theta_0(1+\cos\theta_0))\sqrt{\frac{2\kappa}{W}} + O(\epsilon^2) \qquad (6)$$

$$\frac{2L}{h} = 2\frac{l_0(\theta_0) + l_1(\theta_0)\sqrt{\frac{\kappa}{WA}}}{h_0(\theta_0) + h_1(\theta_0)\sqrt{\frac{\kappa}{WA}}} + O(\epsilon^2) \qquad (7)$$

All coefficients appearing in the last equations are defined in the Appendix.

The main problem in determining W from the experimental data by using eqs 5−7 is that the surface area and volume of the adhered vesicles are not known. We therefore have to make an additional assumption about the shape of the adhering vesicles. Since we are interested in large values of the flattening ratio $2L/h$, the adhering vesicles will mostly belong to the pancake-regime, where their shape can be approximated by a cylinder of height h and

(40) Karatekin, E.; Sandre, O.; Guitouni, H.; Borghi, N.; Puech, P. H.; Brochard-Wyart, F. Cascades of transient pores in giant vesicles: Line tension and transport. *Biophy. J.* **2003**, *84*, 1734−1749.

(41) Chanturiya, A.; Chernomordik, L. V.; Zimmerberg, J. Flickering fusion pores comparable with initial exocytotic pores occur in protein-free phospholipid bilayers. *Proc. Natl. Acad. Sci. U.S.A.* **1997**, *94*, 14423−14428.

(42) Lenz, P.; Johnson, J. M.; Boxer, S. G. Dye induced leakage of adhering vesicles. In preparation.

(43) Tordeux, C.; Fournier, J. B.; Galatola, P. Analytical characterization of adhering vesicles. *Phys. Rev. E* **2002**, *65*, 041912.

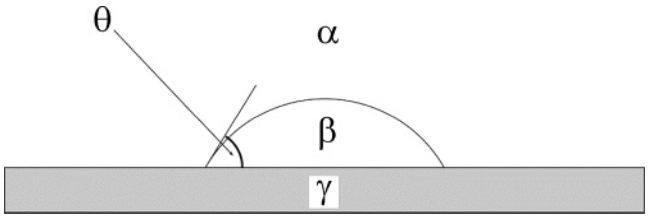

Figure 6. A spherical cap is shown, which is the vesicle shape in the limit of $W \rightarrow \infty$. A droplet of phase β is present on solid γ, surrounded by liquid α. The contact angle θ is defined as the inner angle between the substrate and the tangent to the droplet surface at the contact point.

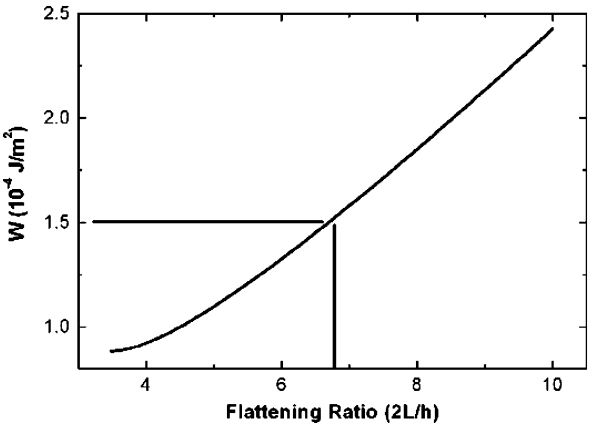

Figure 7. Calculated adhesion potential W as a function of observed flattening ratio, $2L/h$ (where $2L$ = diameter of adsorbed vesicles and h = height). The plot shows the adhesion potential W as calculated from eqs 5−7 for flattening ratios of a given vesicle with radius 50 nm. Guide lines indicate the flattening ratio and estimated adhesion potential for the vesicles investigated.

radius L, which can be measured directly.[28] We thus set eq 5 equal to

$$V = \pi L^2 h \tag{8}$$

and eq 6 equal to

$$A = 2\pi Lh + 2\pi L^2 \tag{9}$$

With these approximations and upon setting the left-hand side of eq 7 equal to the experimentally measured values of $2L/h$, eqs 5 and 6 can be used to solve for the remaining unknowns $(\kappa/W)^{1/2}$ and θ_0. Figure 7 shows the results of this analysis for vesicles with radii $R = 50$ nm and $\kappa \approx 10kT$.

Since our approximation is more accurate for larger vesicles, we selected a subset of vesicles with an adhered width larger than 200 nm. This subset of vesicles has an average flattening ratio of 6.8 ± 2.9, which corresponds to an adhesion potential of $W \approx 1.5 \pm 0.8 \times 10^{-4}$ J/m^2. With this value of W, ϵ^2 is of the order of 0.02 and therefore it is justified to neglect the higher-order terms in the expansion above. However, two additional sources of error may exist: (1) The cylindrical approximation used to determine the area and volume of adhering vesicles may be inaccurate, and (2) deformations due to the AFM tip may increase the measured flattening ratios.[37]

The measured adhesion potential of 1.5×10^{-4} J/m^2 is an order of magnitude smaller than the value previously reported by Reviakine and Brisson for PC vesicles adhered to mica, estimated to be 3.5×10^{-3} J/m^2.[24] Comparison of the AFM force that induces rupture gives a reference point for how strong the adhesion potential is. The rupture force F_c induces a tension in the membrane given by $\sigma = (F_c/\pi r_t^2) l_b$, where r_t is the tip radius and l_b is the thickness of the bilayer. Assuming $r_t = 30$ nm and $l_b = 5$ nm, we find for the measured value of $F_c = 60$ pN that $\sigma \approx 10^{-4}$ J/m^2. The fact that σ is of comparable magnitude to W suggests that the adsorbed vesicles are strongly adhered and only a moderate additional force is required to rupture the vesicles.

Reviakine and Brisson's value for W was taken from a measured critical rupture radius (R_r) of 75 nm using the relation

$$R_r = \frac{2\Lambda - g(2\kappa W)^{1/2}}{W} \tag{10}$$

where Λ is the line tension of the bilayer disk and g is a numerical constant on the order of 1.[24,28] Taking similar values for κ and Λ used by Reviakine et al., 5×10^{-20} J and 1.3×10^{-10} J/m, respectively, our estimated adhesion potential of 1.5×10^{-4} J/m^2 would yield an estimated R_r of approximately 2 μm for PC vesicles on glass. However, values typically reported for Λ are on the order of 2×10^{-11} J/m,[40,44] which yields an R_r of 250 nm for $W \approx 1.5 \times 10^{-4}$ J/m^2. Both these values are above the radius of the vesicles used to estimate W ($R \approx 50$ nm), which is consistent with the fact that no vesicles were observed to undergo isolated rupture to form bilayer disks. Furthermore, if Reviakine et al. had used the value of $\Lambda = 2 \times 10^{-11}$ J/m, they would have estimated an adhesion potential on mica much closer to our estimate for glass ($W \approx 5 \times 10^{-4}$ J/m^2).

Conclusion

Our AFM data show that the adsorption of egg PC vesicles to glass surfaces leads to isolated *intact* vesicles at low concentrations of vesicles in solution. Vesicles labeled with 6% TR also adsorb intact. Taken in conjunction with previous work,[1] these results suggest that 6% TR vesicles form rupture pores but do not fully rupture to form bilayer disks when adsorbed to glass. For increasing vesicle concentrations, there is an increase in surface coverage; however, a coexistence of bilayer disks originating from ruptured vesicles and adsorbed vesicles has *not* been observed. This observation is in contrast to reports of vesicle adsorption on mica, where vesicles of 100 nm diameter in solution were observed to adsorb both as intact vesicles and as bilayer disks.[24] However, our data are in agreement with recent quartz crystal microbalance (QCM) measurements of vesicles on glass, which also showed intact vesicles of 100 nm diameter adsorbing.[27] We have estimated the adhesion energy (W) of egg PC vesicles adsorbed to glass to be on the order of 1.5×10^{-4} J/m^2, which is of the same order of magnitude as the tip-induced tension required for vesicle rupture. We can approximate the critical rupture radius (R_c) as being >250 nm, depending on what value is used for the line tension of a bilayer disk. For high vesicle concentrations, continuous lipid bilayers with a thickness of ~5 nm are formed, which possess no detectable defects.

Acknowledgment. H.S. gratefully acknowledges financial support by the Deutsche Akademischer Austauschdienst (DAAD) in the framework of the "Hochschulsonderprogramm III" and the NSF MRSEC Center

(44) Evans, E.; Heinrich, V.; Ludwig, F.; Rawicz, W. Dynamic tension spectroscopy and strength of biomembranes. *Biophys. J.* **2003**, *85*, 2342−2350.

on Polymer Interfaces and Macromolecular Assemblies (CPIMA) under DMR 9808677. P.L. acknowledges support through the Emmy-Noether program of the DFG and the Otto-Hahn program of the Max-Planck society. S.G.B. acknowledges support from the NSF and NIH.

Supporting Information Available: Top view and cross-sectional analysis of an AFM height image of an adsorbed vesicle; AFM height images of adsorbed, labeled vesicles at increasing solution concentrations; AFM image and section analysis of a scratched bilayer. This material is available free of charge via the Internet at http://pubs.acs.org.

Appendix: Expansion around the Strong Adhesion Limit

In this Appendix, we briefly define the coefficients appearing in eqs 5−7. Surface area and volume of the adhering vesicle are given by[43]

$$A = A_{\mathrm{cap}} - \delta A \tag{A1}$$

$$V = V_{\mathrm{cap}} + O(\epsilon^2) \tag{A2}$$

where

$$V_{\mathrm{cap}}(\theta,R) = \frac{1}{3}\pi R^3[2(1-\cos\theta) - \sin^2\theta\cos\theta] \equiv \frac{1}{3}\pi R^3 \tilde{V}(\theta) \tag{A3}$$

and

$$A_{\mathrm{cap}}(\theta,R) = \pi R^2[2(1-\cos\theta) + \sin^2\theta] \equiv \pi R^2 \tilde{A}(\theta) \tag{A4}$$

and

$$\delta A = 4\pi\left(\cos\frac{\theta}{2} - \cot\frac{\theta}{2}\right)\sqrt{\frac{2\kappa}{W}}L_0 + O(\epsilon^2) \equiv 4\pi\delta\tilde{A}(\theta)\sqrt{\frac{2\kappa}{W}}L_0 + O(\epsilon^2) \tag{A5}$$

where $L_0 = R_0 \sin\theta_0$.

For large (but finite) W, the shape of the vesicles is also characterized by a contact angle θ and radius R given by $\theta = \theta_0 + \delta\theta$ and $R = R_0 + \delta R$. The first order corrections are given by

$$\delta\theta = \frac{2\left(\sin\frac{\theta_0}{2} - 1\right)(2+\cos\theta_0)}{R_0\sin\theta_0}\sqrt{\frac{2\kappa}{W}} + O(\epsilon^2) \equiv \delta\tilde{\theta}(\theta_0)\frac{1}{R_0}\sqrt{\frac{2\kappa}{W}} + O(\epsilon^2) \tag{A6}$$

and

$$\delta R = \frac{2\left(1-\sin\frac{\theta_0}{2}\right)\sin^2\theta_0}{(1-\cos\theta_0)^2}\sqrt{\frac{2\kappa}{W}} + O(\epsilon^2) \equiv \delta\tilde{R}(\theta_0)\sqrt{\frac{2\kappa}{W}} + O(\epsilon^2) \tag{A7}$$

In first order in ϵ, the ratio between L (the radius of the adhesion area of the vesicle) and the height h of the vesicle is given by

$$\frac{L}{h} = \frac{l_0 + l_1\sqrt{\frac{\kappa}{WA}}}{h_0 + h_1\sqrt{\frac{\kappa}{WA}}} + O(\epsilon^2) \tag{A8}$$

where

$$l_0 = \sqrt{\frac{1+\cos\theta_0}{\pi(3+\cos\theta_0)}} \tag{A9}$$

$$l_1 = -\sqrt{2}\frac{\cos\theta_0/2}{1+\sin\theta_0/2} \tag{A10}$$

$$h_0 = \sqrt{\frac{1-\cos\theta_0}{\pi(3+\cos\theta_0)}} \tag{A11}$$

$$h_1 = -2\sqrt{2}\left(1-\sin\frac{\theta_0}{2}\right) \tag{A12}$$

LA049302V